Hindawi
Mathematical Problems in Engineering
Volume 2021, Article ID 9991425, 12 pages
https://doi.org/10.1155/2021/9991425

Research Article

Mechanical Characteristics of Coal and Rock in Mining under Thermal-Hydraulic-Mechanical Coupling and Dynamic Disaster Control

Haifeng Ma,[1,2] **Lingjie Wang**,[2] **Xin'gang Niu**,[2,3] **Fanfan Yao**,[2] **Kexue Zhang**,[1,4] **Jucai Chang**,[2] **Yingming Li**,[2] **Xiangyang Zhang**,[2] **Chaunming Li**,[2] **and Zuxiang Hu**[2]

[1]*Key Laboratory of Safety and High-efficiency Coal Mining, Ministry of Education (Anhui University of Science and Technology), Huainan, Anhui 232001, China*
[2]*School of Mining Engineering, Anhui University of Science and Technology, Huainan, Anhui 232001, China*
[3]*China Coal Technology and Engineering Group Chongqing Research Institute, Chongqing 400037, China*
[4]*School of Safety Engineering, North China Institute of Science and Technology, Langfang, Hebei 101601, China*

Correspondence should be addressed to Lingjie Wang; 2509356841@qq.com and Kexue Zhang; zhkexue@163.com

Received 8 March 2021; Accepted 26 April 2021; Published 7 May 2021

Academic Editor: Chun Zhu

In order to reduce the risk of coal and rock dynamic disasters in the coal mine production process, the coupling mechanics characteristics of coal and rock produced in the process of coal mining in the Dingji Coal Mine are taken as the research object, and the experimental study on the deformation characteristics and the variation rule of mechanical parameters of raw coal under multifield coupling (temperature, gas, and stress coupling) was carried out. The results show that the elastic modulus, peak strain, and peak stress of raw coal samples under the thermal-hydraulic-mechanical coupling have the same change law in the test temperature range and all of them show a linear decreasing law as the temperature increases. Under the same temperature gradient increasing condition, the elastic modulus, peak strain, and peak stress show a nongradient decreasing trend as the temperature increases. Both the deformation modulus and the lateral expansion coefficient show a linear increase as the temperature increases, while the deformation modulus and the lateral expansion coefficient show a nongradient increase trend as the temperature increases under the same temperature gradient increasing condition. Under the action of the thermal-hydraulic-mechanical coupling, unloading confining pressure obviously accelerated the yield process of the coal sample, and the confining capacity of confining pressure on transverse strain of the coal sample decreased. To prevent the occurrence of coal and gas outburst, it is necessary to take specific prevention measures according to the change law of triaxial compression mechanics of a raw coal specimen under the action of the thermal-hydraulic-mechanical coupling.

1. Introduction

Coal and rock are generally in an environment where stress, temperature, and other factors act together, especially in deep high-gas mines. The mechanical behavior of coal and rock is mainly influenced by coupling effects of stress, temperature, gas, and other factors, as shown in Figure 1.

The stress state of rock mass and coal under the mining condition is relatively complex, which shows the comprehensive effect of loading and unloading, that is, loading in the axial direction and unloading in the radial direction. With the advance of the working face, the stress state of the coal body in front of the working face will change, and it will experience the combined action of complex loading and unloading.

Scholars at home and abroad have made great achievements in permeability of coal or rock mass, deformation law of coal or rock under different loading and unloading paths, and strength characteristics.

A coupled thermal-hydraulic-mechanical-chemical model was proposed and upgraded, which could describe the chronic evolution of the permeability of rock because of

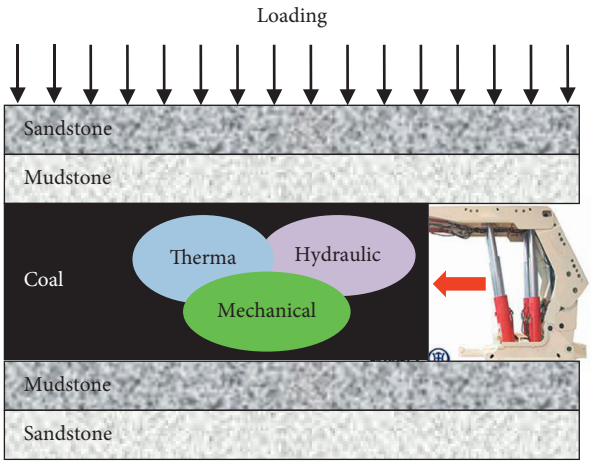

Figure 1: Schematic diagram of thermal-hydraulic-mechanical coupling.

mineral reactions within rock fractures [1]. To search the occurrence law and mechanism of complicated dynamic disasters in deep underground coal mines, a new experimental method was proposed, and the tests of effects of different loading rates on the complicated dynamic disaster under the condition of true-triaxial stress environment were carried out [2]. To investigate the deformation and destroyed law of combined sample with different ratios of coal and rock, uniaxial compression plan experiments on sandstone, coal, and other three kinds of combined samples were designed and carried out [3]. To probe the mining mechanical response laws of coal and rock with different burial depths, the differences of deformation characteristics and mining stress of the coal and rock with five different burial depths were researched based on field initial geostress data, laboratory testing results and the geological conditions [4]. The movement laws and destroyed characteristics of the overlying rock strata under the condition of mining were researched by using a similar material simulation test based on the actual geological and mining conditions of a coal mine in Inner Mongolia [5]. Due to the unique mining spatial structure, the distribution characteristics of mining stress of the isolated island working face were necessary to explore based on a specific engineering example; a structural mechanical model of the overlying rock strata (as continuous beam) was established by using elastic-plastic mechanics theory, and the destroyed depth of coal and rock mass and the mechanical equations of the mining stress were obtained [6].

To probe the differences of deformation characteristics and destroyed behavior of coal with different burial depths in the process of coal mining, the triaxial loading and unloading tests with acoustic emission monitoring were carried out on coal samples with four different burial depths, which were taken from the Pingdingshan Coal Mine area [7]. The mineral composition, elemental contents, and mesostructures and microstructures of 16 kinds of sandstone, which were taken from three coal mines, were researched by polarizing microscope analysis and X-ray diffraction, and the conclusion was obtained that the cohesion, elastic modulus, friction coefficient, and the strength all increased with the increase in the degree of particle contact and quartz content [8]. The dynamic impact mechanical characteristics of coal with anisotropic structure at low and medium strain rates were researched through a self-developed vertical Split Hopkinson Bar equipment, and the strain rate, dynamic elastic modulus, destroyed characteristics, and peak stress of raw coal were analyzed under the influence of structural anisotropy and five-impact loading [9]. The change characteristics of mineral composition, microscopic fracture characteristics, and mechanical properties of Sichuan sandstone, which was treated at 600 degrees C, were researched through various techniques and methods [10].

Triaxial unloading confining pressure experiments under the condition of different unloading rates and different initial confining pressures were carried out, which were to study the influence of the unloading path on the mechanical properties of coal, and the experimental result showed that the coal samples were easily destroyed under the condition of unloading [11]. The deformation characteristics and stress of coal and rock combined bodies were analyzed based on triaxial compression experiments of coal and rock combined bodies with different height ratios, and the strength reduction coefficient, elastic modulus, and peak stress of the coal and rock combined body were negatively correlated with the ratio of coal and rock combination height [12]. A uniaxial compression test of rock samples with different water content rates, which were taken from the Ruineng coal mine in Yan'an city, was carried out, and the effect of water content rates on acoustic emission of rock samples was clarified [13]. Layered cemented paste backfill (CPB) samples with different layers were prepared, three cycles of four confining pressures were designed, and the experiment on microstructural characteristic and mechanical properties of CPB under the condition of triaxial cyclic loading and unloading was carried out [14]. The rockburst experiments, which, on the evolution laws of temperature field during rockburst, effected by gradient stress, under the condition of true-triaxial gradient loading were carried out by using a hydraulic-pneumatic-gradient composite loading true-triaxial test system [15].

The three-axis loading-unloading-uniaxial reloading mechanical tests on white sandstone specimens under the condition of different initial axial pressures and confining pressures, to research the problem of deformation and failure caused by rock unloading during excavation, were carried out, and the weaken mechanisms and damage of white sandstone specimens during uniaxial reloading, triaxial loading, and unloading were analyzed [16]. The destroyed modes of lightweight concrete were changed, and the impact resistance of it was significantly improved under the condition of static-dynamic and load coupled effect, and the stress-strain curve at higher strain rate could be divided into five stages [17]. The experiment on damage evolution of sandstone under the condition of loading and unloading was carried out, which was to judge the stress state of bedrock in engineering and provide a theoretical basis for complex rock engineering [18]. The experiment on the damaged and seepage characteristics of gas-bearing coal under the

condition of loading and unloading was carried out, which was to probe the effects of accelerated advancement of the working face [19]. A series of saturated sandstones were made, and the experiment on postpeak cyclic loading and unloading was carried out, which was to research the mechanical properties of saturated sandstones [20].

Experiment of coal samples under the condition of true-triaxial loading and unloading was carried out, and the energy evolution, fracture characteristics, and stress characteristics were analyzed, and the coal burst breeding and mechanical mechanisms of coal samples were revealed [21]. Triaxial unloading experiment under the condition of different stress paths was carried out, which was to research the mechanical properties of shale rock under unloading [22]. Cyclic loading-unloading tests were carried out, which was to study the energy evolution characteristics and mechanical properties of impact-prone coal, and the acoustic emission signals and stress and strain data were obtained [23]. The connection direction and development of cracks was inhibited due to increase of confining pressure and the length of the final fracture surface was decreased, and at the same time, the development of radial irreversible strain was reduced [24]. Triaxial cyclic loading-unloading experiments were carried out, which was to research the effect of cyclic loading-unloading on coal seams in the progress of mining, and the dissipated energy ratio and the permeability recovery rate were defined to analyze the evolution laws of deformation, energy, and permeability [25].

Uniaxial and true-triaxial compression tests were carried out on red sandstone samples with saturated water content and different water contents, which was to study the effects of water on energy, stress, and fracture characteristics of rock damaged in a hard-rock tunnel [26]. Several experiments were conducted based on self-developed equipment for visual gas-solid coupling mechanics, which was to study the crack propagation behavior and the changes observed in the stress-strain, and the dissipated energy and the fractals of fragments were analyzed [27]. The blasting vibration signals monitored at a blasting site were used to investigate the attenuation characteristics of blasting vibration through the energy distribution, frequency characteristics, and peak particle velocity of the blasting vibration signals analyzed through the time-frequency processing method [28]. The dynamic compressive behavior of gas-containing coal with static axial preloading and gas pressure was researched through a modified Split Hopkinson Pressure Bar system, and the dynamic behavior of gas-containing coal under SHPB tests was studied by varying axial static preloading and initial gas pressure [29]. Two types of experiments were conducted under the condition of different boundaries, which was to examine the anisotropic deformation and study the directional permeability and anisotropic deformation of the coal sample [30]. A physical model of negative Poisson's ratio cable, fracture evolution and energy characteristics during marble failure, permeability evolution of two-dimensional fracture networks during shear, the bolt-grouting design evaluation method, dynamic stability evaluation of underground cavern sidewalls, and the safe mining depth of antidip bedding slope was studied [31–37]. The true-triaxial compression tests were performed on red sandstone cubic specimens with a circular hole for investigating the influence of depth on spalling in tunnels [38].

In summary, there are few research results on the mechanical behavior of deep coal and rock under the effect of THM coupling. In this paper, the deep high-temperature coal seam is taken as the research object, and the test conditions of different temperatures, gas pressures, and stress environments are set to study the mechanical behavior characteristics of coal seam under multifield coupling in the mining process, so as to provide reference for the design and construction of deep coal seam mining.

2. Overview of the Coal Mine

The Dingji Coal Mine (Figure 2) of Huaihu Coal Power Co., Ltd. is located in Fengtai County, Anhui Province, about 50 km away from Huainan city, with superior geographical location and convenient transportation. The field is 14.75 kilometers long from east to west and 11 kilometers wide from north to south. The mine has a geological reserve of 1.279 billion tons and exploitable reserves of 640 million tons. There are nine coal seams in the mine with stable occurrence of coal seams. The mine has a designed production capacity of 5 million tons per year and was put into operation on December 26, 2007. The first-level elevation of the mine is −826 m, and the western auxiliary level is −910 m.

The observation data of drilling temperature shows that the floor temperature of the main workable coal seam increases with the increase of its depth in the Dingji Coal mine. The ground temperature variation range of mine depth −500 m is between 20 and 35.5°C. The ground temperature below −600 m is above 38°C, and the rock temperature at the bottom of the well is above 40°C. The geothermal gradient of the whole well field was 2.3~4.1°C/hm, with an average of 3.2°C/hm, belonging to the secondary heat damage area. In the summer of 2008, when the surface temperature was 27°C, the back flow air temperature of the mining face of the 11-2 coal seam was as high as 37°C. Some borehole geothermal data are shown in Table 1.

3. Methodology

3.1. The Test System. The experimental system is mainly composed of a host machine, a servo loading system, a three-axis pressure chamber, a water temperature control system, a pneumatic control system, a data acquisition system, and a safety protection system. The main components are shown in Figure 3. The test system can be used to carry out mechanical tests under various loading environments, such as compression, shear, creep, and high temperature of geotechnical engineering materials, concrete, and other artificial materials.

The main performance indexes of the servo loading system are as follows:

(1) Axial compression force ≤1459 kN, axial tensile force ≤961 kN, and maximum stroke of the actuator 100 mm

Figure 2: Dingji Coal Mine, Huai Hu Coal Power Co., Ltd.

Table 1: Partial drilling ground temperature data.

Hole number	Hole depth (m)	Bottom rock temperature (°C)	Geothermal gradient (°C·hm^{-1})
16-4	874.3	44.9	3.7
16-6	833.38	46.1	3.6
20-4	910.45	50.2	3.8
847	906.46	51.8	4
23-14	1034.49	52.7	3.4

Figure 3: Main components of the rock mechanics test system.

(2) Maximum test space: height: 782 mm, width: 724 mm

(3) Shear actuator output, extending 261 kN, pumping 167 kN, stroke: 100 mm, and shear specimen: 150 × 150 × 300 mm

(4) Stiffness: 777 kN/mm

(5) Power of hydraulic source (HPS): 18 kW

(6) Hydraulic source flow: 26.5 L/min

(7) Output waveform: square wave, sine wave, straight line, half sine wave, arbitrary regular curve waveform, and random waveform

3.2. Specimen Preparation. Coal samples used in this test are taken from the 1231(1) working face of transportation roadway in coal seam 11-2 of the Dingji Coal Mine. The average thickness of the coal seam is 2.5 m, the average dip angle is 5°, and the buried depth is 750 m. The original gas pressure of the coal seam is 1.0 MPa. The coal collected at the heading face is well preserved and sent to the laboratory. The coal size is no less than 20 cm × 20 cm × 20 cm. A core drilling machine is used to drill a raw coal pillar of 50 mm diameter, and the high-speed cutting machine is adopted to the raw coal pillar for cutting, grinding, making face parallelism conform to the requirements of the test, and making size for the Φ 50 mm × 100 mm standard specimen. As shown in Figure 4, the prepared raw coal specimens shall be dried in an oven and stored in a drying oven after being cooled to room temperature for testing purposes.

3.3. Test Plan. In order to obtain the mechanical characteristics of coal and rock under the action of thermal-hydraulic-mechanical coupling, the experimental study on the mechanical behavior of coal and rock under the condition of loading and unloading was carried out using an MTS816 electrohydraulic servo rock mechanical test system. In the test, vertical stress and horizontal stress are simulated by axial pressure and confining pressure, respectively; that is, the mechanical behavior of coal and rock under mining disturbance is simulated by increasing axial pressure and decreasing confining pressure.

The gas pressure in this test was 1.0 MPa, and methane with pure concentration of 99.99% was used as the test gas. The test temperature was divided into 5 levels, namely, 30°C, 40°C, 50°C, 60°C, and 70°C. Mechanical tests on loading and unloading of coal and rock were carried out at different temperatures. Specific steps are as follows: (1) first, $\sigma 1 = \sigma 3(\sigma 2)$ is applied gradually to a predetermined value (15 MPa) under hydrostatic pressure. (2) Then, the raw coal specimens were filled with methane, and under the condition of methane pressure of 1.0 mpa, the raw coal specimens

Figure 4: Partial specimens.

reached the equilibrium of adsorption and desorption. (3) The confining pressure was discharged at a rate of 0.001 MPa/s until the target value (2 MPa), and the axial pressure was applied by force control. The axial pressure was increased until the specimen failed. After the failure, the specimen was loaded at a speed of 0.1 mm/min in displacement control, until the residual strength of the specimen was basically stable. The stress path is shown in Figure 5.

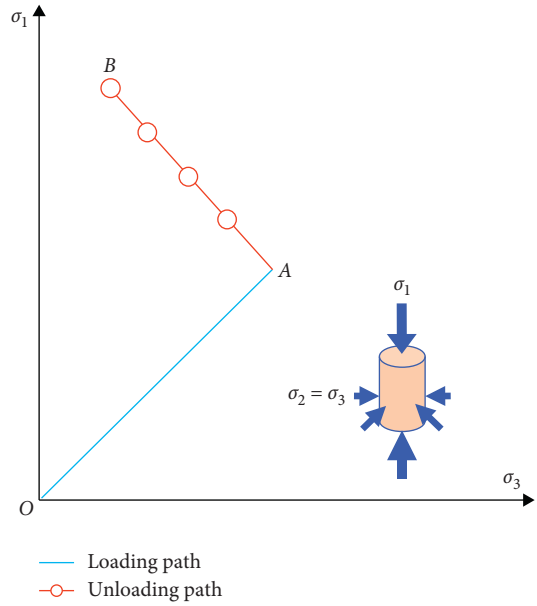

Figure 5: Schematic diagram of stress loading and unloading path.

4. Result Analysis and Discussion

4.1. Characteristics of the Stress-Strain Curve in the Whole Process under the Action of THM Coupling. Under the action of thermal-hydraulic-mechanical coupling, the total stress-strain curve of raw coal sample 11-2 in the triaxial mechanical test is shown in Figure 6 (take specimen 11-30-A3 as an example). The triaxial stress-strain curve of the raw coal specimen is basically consistent with the conventional stress-strain curve, which successively goes through four stages of compaction deformation, elastic deformation, plastic deformation, and residual deformation failure.

Table 2 shows the peak stress, peak axial strain, volumetric strain, Poisson's ratio, radial strain, and other results of the triaxial mechanical test of raw coal sample 11-2 under the action of thermal-hydraulic-mechanical coupling. In order to analyze the discrete characteristics of the loading and unloading triaxial mechanical test results of the raw coal specimen under the action of thermal-hydraulic-mechanical coupling, a mathematical statistics method is adopted to conduct statistical analysis of the test results according to the following formula:

$$\overline{x} = \frac{1}{n}\sum_{i=1}^{n} x_i,$$

$$S = \sqrt{\frac{1}{n}\sum_{i=1}^{n}(x_i - \overline{x})^2}, \tag{1}$$

$$\xi = \frac{S}{\overline{x}}.$$

In the formula, $\overline{x}$ refers to the average, S refers to the standard variance, and ξ refers to the coefficient of variation.

It can be seen from Figure 6 and Table 2 that the stress-strain curve changes linearly at the elastic deformation stage. As the temperature increases, the elastic stage of the curve moves to the left gradually, and the slope decreases accordingly, that is, the average elastic modulus decreases. The yield stage is the stage before the raw coal specimen is about to be destroyed. When the temperature is low, the yield stage is short, and the specimen enters the residual deformation stage once the yield reaches its ultimate strength; when the temperature is high, the yield stage is relatively obvious, and the stress will still increase before the ultimate strength is reached. In the stage of residual deformation and failure, when the temperature is below 40°C, the specimen as a whole

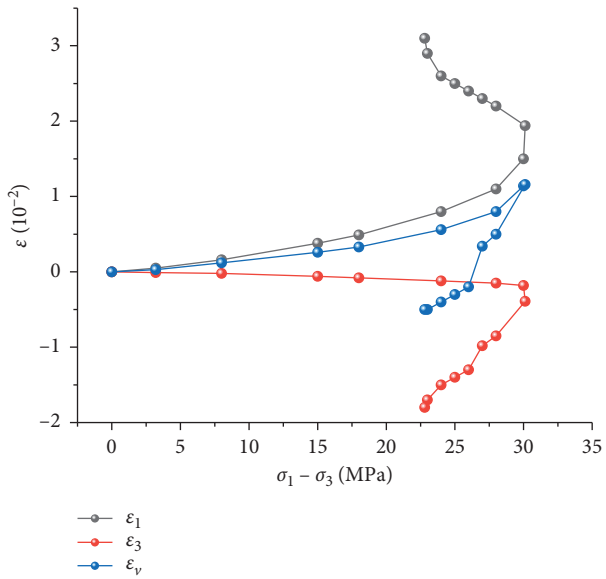

Figure 6: Stress-strain curve (11-30-A3).

Table 2: Triaxial loading and unloading test results of the raw coal specimen.

Number	Temperature (°C)	Gas pressure (MPa)	σ_1 (MPa)	σ_3 (MPa)	At peak stress			
					ε_1 (10^{-2})	ε_3 (10^{-2})	ε_v (10^{-2})	μ
11-30-A1			31.08	2.95	1.75	−0.41	0.93	0.234
11-30-A2	30	1.0	32.16	3.01	1.88	−0.48	0.92	0.255
11-30-A3			33.27	3.15	1.94	−0.39	1.16	0.201
Mean			32.17	3.04	1.86	−0.43	1.00	0.230
Standard deviation			0.894	0.084	0.079	0.039	0.111	0.022
Coefficient of variation			0.028	0.028	0.043	0.090	0.110	0.097
11-40-B1			30.02	3.26	1.71	−0.41	0.89	0.240
11-40-B2	40	1.0	29.85	3.21	1.64	−0.39	0.86	0.238
11-40-B3			28.96	3.18	1.62	−0.37	0.88	0.228
Mean			29.61	3.22	1.66	−0.39	0.88	0.235
Standard deviation			0.465	0.033	0.039	0.016	0.012	0.005
Coefficient of variation			0.016	0.010	0.023	0.042	0.014	0.021
11-50-C1			26.85	3.37	1.49	−0.35	0.79	0.235
11-50-C2	50	1.0	27.63	3.34	1.53	−0.37	0.79	0.242
11-50-C3			28.57	3.29	1.60	−0.38	0.84	0.238
Mean			27.68	3.33	1.54	−0.37	0.81	0.238
Standard deviation			0.703	0.033	0.045	0.012	0.024	0.003
Coefficient of variation			0.025	0.010	0.030	0.034	0.029	0.012
11-60-D1			26.56	3.42	1.42	−0.35	0.72	0.246
11-60-D2	60	1.0	25.89	3.38	1.35	−0.33	0.69	0.244
11-60-D3			25.75	3.34	1.32	−0.31	0.70	0.235
Mean			26.07	3.38	1.36	−0.33	0.70	0.242
Standard deviation			0.353	0.033	0.042	0.016	0.012	0.005
Coefficient of variation			0.014	0.010	0.031	0.049	0.018	0.021
11-70-E1			25.01	3.48	1.14	−0.30	0.54	0.263
11-70-E2	70	1.0	24.78	3.45	1.11	−0.27	0.57	0.243
11-70-E3			23.95	3.41	1.06	−0.25	0.56	0.236
Mean			24.58	3.45	1.10	−0.27	0.56	0.247
Standard deviation			0.455	0.029	0.033	0.021	0.012	0.012
Coefficient of variation			0.019	0.008	0.030	0.075	0.022	0.047

will fail soon after reaching the peak stress, and the residual stress will be small. When the temperature is higher than 40°C, the specimen as a whole will fail slowly after reaching the peak stress, the stress gradually decreases, and the postpeak residual stress is larger.

When the temperature was 30°C and 50°C, the prepeak curve of each specimen had the same trend of change, but the peak stress was relatively discrete, and the coefficient of variation was 0.028 and 0.025, respectively. When the temperature was 40°C, 60°C, and 70°C, the stress-strain curves of the specimens changed in a similar way, and their coefficients of variation were 0.016, 0.014, and 0.019, respectively.

The deformation of linear elastic materials is usually described by two parameters of Hooke's law (elastic modulus E and Poisson's ratio μ). In the triaxial compression experiment with constant confining pressure, these two parameters are calculated by the following formula:

$$E = \frac{d\sigma_1}{d\varepsilon_1}, \quad \mu = \frac{d\varepsilon_3}{d\varepsilon_1}. \tag{2}$$

In the formula, σ_1 refers to the axial compression, σ_3 refers to the confining pressure, ε_1 is the axial strain, ε_3 is the radial strain, E is the elastic modulus, and μ refers to Poisson's ratio.

Since coal and rock are nonlinear elastic materials, in the whole stress-strain process, the elastic modulus of coal and rock will evolve with the change of deformation. Therefore, it is inappropriate to use Hooke's law to describe the deformation of coal and rock. In the triaxial compression experiment with relief of confining pressure, the confining pressure is constantly changing. In order to consider the influence of confining pressure changes, the deformation modulus E_0 and the lateral expansion coefficient μ_0 in the whole stress-strain process are defined [39].

$$E_0 = \frac{\sigma_1 - \sigma_3}{\varepsilon_1}, \quad \mu_0 = -\frac{\varepsilon_3}{\varepsilon_1}. \tag{3}$$

In the formula, E_0 refers to the deformation modulus, μ_0 refers to the lateral expansion coefficient, and σ_1–σ_3 refers to the deviatoric stress.

The whole process curve of deviator stress-axial strain can be roughly divided into an elastic stage, yield stage, plastic deformation stage, and residual stress stage. After the unloading of confining pressure begins, the deviator stress-axial strain curve of the coal sample enters into the yield section rapidly. Under the condition of discharging confining pressure, the yield section of the coal sample is shortened obviously, and the peak stress and corresponding axial strain are decreased significantly. It can be seen that the release of confining pressure significantly accelerates the yield process of the coal sample because the lower the confining pressure is, the lower the compressive strength and deformation resistance of the coal sample will be.

4.2. Characteristics of Peak Stress under Thermal-Hydraulic-Mechanical Coupling. Figure 7 shows the change curve of peak stress with temperature of the raw coal specimen under triaxial compression.

It can be seen from Figure 7 that the peak stress of raw coal specimen in the test temperature range shows a decreasing trend as the temperature increases, and the fitting formula of the relation curve between average peak stress and temperature is that $\sigma_1 = 37.38 - 0.19t (R^2 = 0.983)$, where t refers to temperature.

Under the same temperature gradient increasing condition, the peak stress shows a nongradient decreasing trend as the temperature increases. When the temperature is 30°C, 40°C, 50°C, 60°C, and 70°C, the corresponding average peak stress is 32.17 MPa, 29.61 MPa, 27.68 MPa, 26.07 MPa, and 24.58 MPa, respectively, and the average peak stress decreases by 2.56 MPa, 1.93 MPa, 1.62 MPa, and 1.49 MPa in turn, and the decreasing range is 7.96%, 6.51%, 5.84%, and 5.70% in turn. In the process of rising temperature, the mineral composition of the specimen is continuously decomposed, and the internal structure of the specimen is damaged, which makes the peak stress of the specimen gradually decrease. At the same time, the raw coal specimen contains adsorbed and free gas, and under the joint action of rising temperature and gas pressure, the strength of the raw coal specimen decreases.

4.3. Peak Strain Characteristics under THM Coupling. Figure 8 shows the change curve of peak strain with temperature of the raw coal specimen under triaxial compression.

It can be seen from Figure 8 that the peak strain of the raw coal specimen in the test temperature range decreases as the temperature increases, and the fitting formula of the relationship between average peak strain and temperature is that $\varepsilon_1 = 2.40 - 0.02t (R^2 = 0.978)$.

Under the same temperature gradient increasing condition, the peak strain shows a nongradient decreasing trend as the temperature increases. When the temperature is 30°C, 40°C, 50°C, 60°C, and 70°C, the corresponding average peak strain is 1.86, 1.66, 1.54, 1.36, and 1.10, respectively, the average peak strain decreases by 0.20, 0.12, 0.18, and 0.26 in turn, and the decreasing range is 10.77%, 7.04%, 11.47%, and 19.07% in turn. As the temperature increases, the moisture content in the specimen decreases gradually, the internal void closes gradually, and the longitudinal deformation decreases gradually, resulting in the peak strain decreasing as the temperature increases.

4.4. Characteristics of Elastic Modulus under the Action of THM Coupling. Figure 9 shows the change curve of the elastic modulus of raw coal under triaxial compression with the change of temperature.

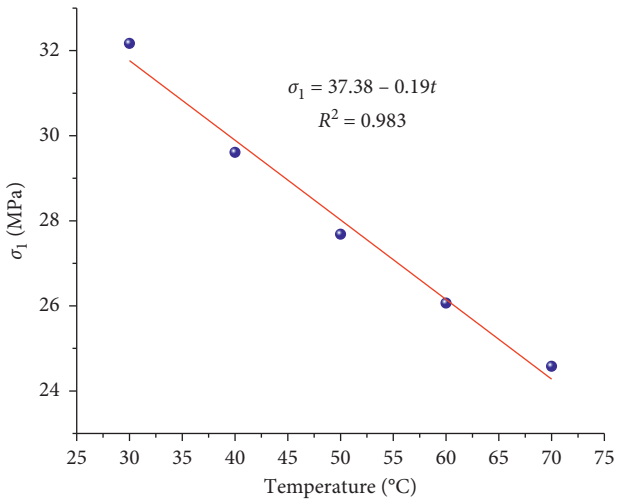

Figure 7: Relation curve between temperature and peak stress.

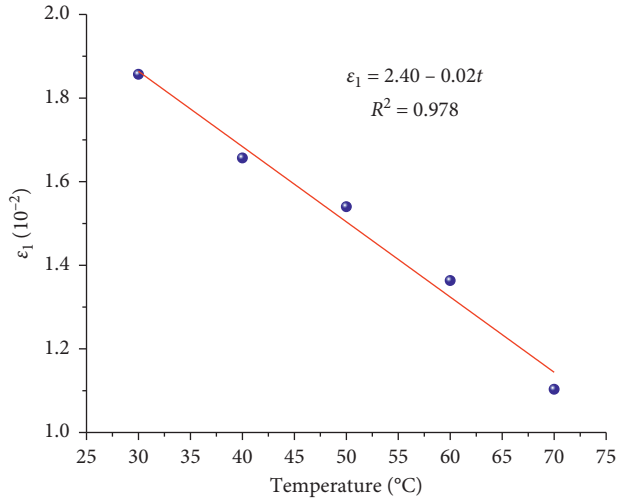

Figure 8: Relation curve between peak strain and temperature.

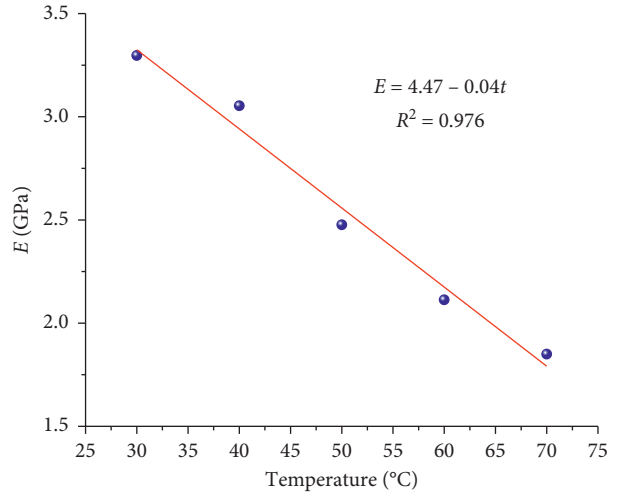

Figure 9: Relation curve between elastic modulus and temperature.

As can be seen from Figure 9, the elastic modulus of the raw coal specimen decreases as the temperature increases within the test temperature range. The fitting formula of the relation curve between mean elastic modulus and temperature is that $E = 4.47 - 0.04t (R^2 = 0.976)$.

Under the same temperature gradient increasing condition, the elastic modulus presents a nongradient decreasing trend as the temperature increases. When the temperature is 30°C, 40°C, 50°C, 60°C, and 70°C, the corresponding average elastic modulus is 3.30 GPa, 3.05 GPa, 2.48 GPa, 2.11 GPa, and 1.85 GPa, respectively, the average elastic modulus decreases by 0.24 GPa, 0.58 GPa, 0.36 GPa, and 0.26 GPa in turn, and the decreasing range is 7.38%, 18.89%, 14.67%, and 12.46% in turn. When the temperature is high, the thermal expansion coefficient of the mineral particles in the raw coal specimen increases, resulting in tensile stress or compressive stress between the particles. When the thermal stress exceeds the contact force between the particles, cracks will be generated and propagated. The deformation of the raw coal specimen increases, leading to a gradual decrease of the elastic modulus.

4.5. Characteristics of the Lateral Expansion Coefficient and Deformation Modulus under the Action of THM Coupling. The deformation modulus can reflect the overall deformation of coal and rock. Figures 10 and 11 show the relation curves of the lateral expansion coefficient, deformation modulus, and temperature, respectively, and Figure 12 shows the relation curves of the lateral expansion coefficient, deformation modulus, and axial strain.

Figures 10–12 show that the deformation modulus of the raw coal specimen gradually increases as the temperature increases, indicating that the overall deformation of the raw coal specimen increases as the temperature increases. Under the same temperature gradient increasing condition, the deformation modulus presents a nongradient increasing trend as the temperature increases. When the temperature is 30°C, 40°C, 50°C, 60°C, and 70°C, the corresponding average deformation modulus is 0.73 GPa, 0.87 GPa, 0.99 GPa, 1.21 GPa, and 1.32 GPa, respectively, and the average deformation modulus increases by 0.14 GPa, 0.12 GPa, 0.22 GPa, and 0.11 GPa in turn, and the increasing range is 19.18%, 14.18%, 22.15%, and 9.07% in turn. The deformation modulus increased from 0.73 GPa at 30°C to 1.32 GPa at 70°C, with an increase of 0.59 GPa and an increase of 80.82%. The overall relationship between deformation modulus and temperature is linear, and its fitting formula is that $E_0 = 0.26 + 0.15t (R^2 = 0.986)$.

The deformation modulus reflects the overall deformation of the specimen during loading and unloading. Coal is generally a special rock with small strength. As the temperature increases, the rheological phenomenon of the specimen becomes more obvious, which leads to the gradual increase of the overall deformation of the specimen.

The lateral expansion coefficient-axial strain curve can be divided into three stages: slow increase, sharp increase, and gentle evolution. After the unloading of confining pressure begins, the curve of lateral coefficient of expansion axial strain of coal sample accelerates rapidly until the coal sample loses its

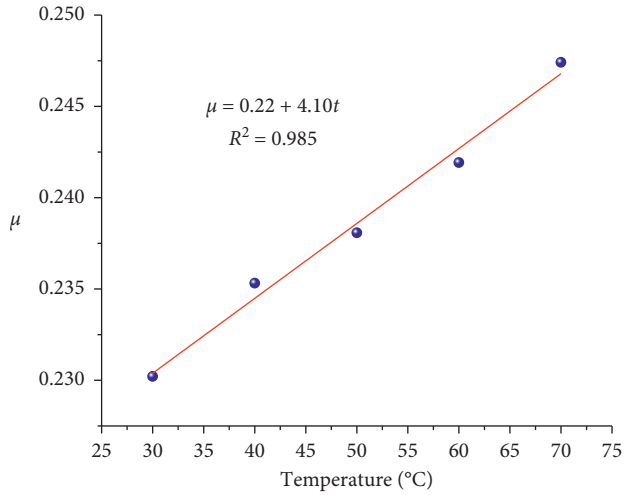

Figure 10: Relation curve between the lateral expansion coefficient and temperature.

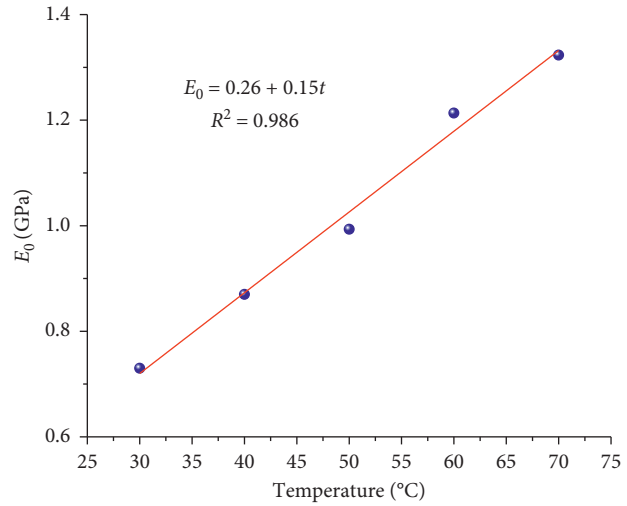

Figure 11: Relation curve between the deformation modulus and temperature.

stability and the lateral coefficient of expansion enters the stage of gentle evolution. The evolution process of the coal sample's lateral expansion coefficient is accelerated obviously by discharging confining pressure. The reason is that, after discharging the confining pressure, its ability to restrain the lateral strain of coal samples also decreases, which leads to the increase of the lateral expansion coefficient.

The evolution trend of deformation modulus-axial strain curve can be roughly divided into four stages: a decreasing stage, slowly increasing stage, rapidly decreasing stage, and gently evolving stage. After unloading confining pressure, the deformation modulus-axial strain curve of coal and rock is suddenly "upward," the slope increases sharply, and the deformation modulus gradient under the corresponding axial strain increases significantly. The reason is that, after the

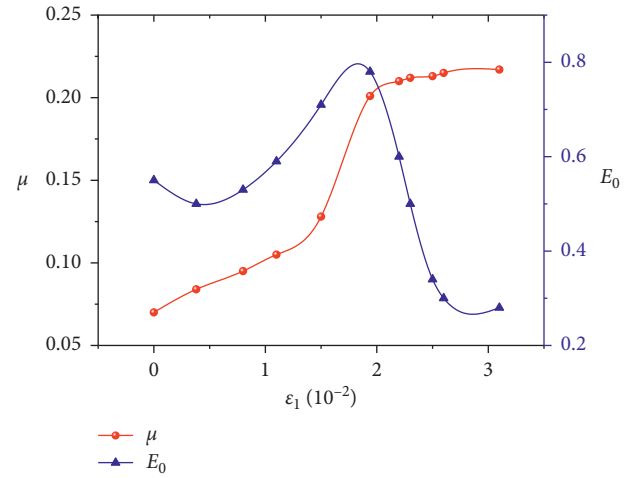

Figure 12: Relation curves of lateral expansion coefficient, deformation modulus and axial strain.

unloading of confining pressure, when the confining pressure decreases, the axial pressure continues to increase, which causes the accelerated increase of deformation modulus, thus resulting in the phenomenon of "upward" of the deformation module-axial strain curve. Under the condition of unloading confining pressure, the deformation modulus of the coal sample enters the rapidly decreasing stage earlier.

4.6. Discussion. By analyzing the results of the triaxial compression mechanics test of the raw coal specimen under the action of thermal-hydraulic-mechanical coupling, it can be seen that, during the triaxial compression test, due to the joint action of temperature and gas, the mechanical characteristics of the raw coal specimen show different characteristics from the conventional triaxial mechanics. Under the action of thermal-hydraulic-mechanical coupling, the elastic modulus, peak strain, and peak stress of the raw coal specimen gradually decrease as the temperature increases, and the decrease trend is approximately linear. The deformation modulus and lateral expansion coefficient increase gradually as the temperature increases, and the increasing trend is approximately linear.

Coal and gas outburst mines have a high risk of coal and gas outburst and gas explosion during the generation process. In the mining process of coal seam, the main energy of instability failure comes from the transformed kinetic energy released by the elastic energy in the coal seam, and this energy value is related to the deformation modulus of coal seam. The smaller the deformation modulus of the coal seam is, the less the elastic energy stored around the working face is and the lower the risk of outburst.

According to the abovementioned analysis, with the increase of coal mining depth, formation temperature rises gradually. As the temperature increases, the strength of coal sample decreases, that is, the stress of coal failure is less. Also,

the influence of rising temperature on the strength and deformation of the coal seam is bound to increase the risk of coal and gas outburst and other dynamic disasters.

5. Engineering Practice

The high-temperature environment of deep mining requires higher prevention and control of coal and gas outburst. In order to avoid the occurrence of coal and gas outburst and other dynamic disasters, it is necessary to take targeted prevention measures according to the change law of triaxial compression mechanics of the raw coal specimen under the action of thermal-hydraulic-mechanical coupling.

Based on the mechanical characteristics of raw coal specimens under thermal-hydraulic-mechanical coupling, during coal seam mining, especially in deep coal seams, the support strength of the excavation roadway should be strengthened, such as increasing the bolt pretightening force and increasing the bolt diameter, reducing the spacing between bolts in special sections, and other measures, to improve the bearing capacity of coal and rock and control the deformation of the roadway during coal mining.

In the mining face with higher temperature, measures such as strengthening ventilation or increasing cold air should be taken to reduce the temperature of coal and rock in the mining space and improve the strength of coal and rock.

Measures, such as strengthening the support strength of the mining roadway and reducing the temperature, were taken in the mining process of the 1231(1) working face in the Dingji Coal Mine, and there were no coal and rock dynamic disaster accidents occurred during the mining period, which effectively guaranteed the safe production of the coal mine.

6. Conclusions

(1) Under the action of thermal-hydraulic-mechanical coupling, the elastic modulus, peak strain, and peak stress of raw coal specimens in the test temperature range all show a linear decreasing trend as the temperature increases, while under the same temperature gradient increasing condition, the elastic modulus, peak strain, and peak stress show a nongradient decreasing trend as the temperature increases.

(2) Under the action of hot-flux-solid coupling, both the deformation modulus and the lateral expansion coefficient of the raw coal specimens in the test temperature range show a linear increase as the temperature increases, while under the same temperature gradient increasing condition, the deformation modulus and the lateral expansion coefficient show a nongradient increase trend as the temperature increases.

(3) Under the action of thermal-hydraulic-mechanical coupling, the yield process of the coal sample is accelerated obviously by discharging confining pressure, and the deformation modulus of the coal sample enters the rapid reduction stage earlier under the condition of discharging confining pressure. The confining capacity of confining pressure to transverse strain of the coal sample decreases, which leads to the increase of deformation modulus and lateral expansion coefficient.

(4) With the increase of coal mining depth, formation temperature rises gradually. As the temperature increases, the strength of the coal sample decreases, that is, the coal reaches the stress of failure and becomes less. The high temperature environment of deep mining requires higher prevention and control of coal and gas outburst. In order to prevent the occurrence of coal and gas outburst and other dynamic disasters, it is necessary to take specific prevention measures according to the change law of triaxial compression mechanics of the raw coal specimen under the action of thermal-hydraulic-mechanical coupling.

Data Availability

The data used to support the findings of this study are included within the article.

Conflicts of Interest

The authors declare that they have no conflicts of interest.

Acknowledgments

This paper was financially supported by the National Natural Science Foundation (51904010, 51774009, 51874002, and 51874006), Natural Science Research Project of Colleges and Universities in Anhui Province (KJ2017A093), Anhui Provincial Natural Science Foundation (1808085QE149, 1808085ME159, 2008085ME142, and 2008085ME147), and Open Foundation from Key Laboratory of Safety and High-efficiency Coal Mining, Ministry of Education (JYBSYS2017105).

References

[1] O. Sho, Y. Hideaki, K. Naoki et al., "Coupled thermal-hydraulic-mechanical-chemical modeling for permeability evolution of rocks through fracture generation and subsequent sealing," *Computational Geosciences*, vol. 24, no. 5, pp. 1845–1864, 2020.

[2] L. Jun, Z. Dongming, H. Gun et al., "Effects of loading rate on the compound dynamic disaster in deep underground coal mine under true triaxial stress," *International Journal of Rock Mechanics and Mining Sciences*, vol. 134, p. 104453, 2020.

[3] Y. Ke, W. Zhen, C. Xiaolou et al., "Experimental research on the mechanical characteristics and the failure mechanism of coal-rock composite under uniaxial load," *Advances in Civil Engineering*, vol. 2020, Article ID 8867809, 11 pages, 2020.

[4] Z. Ersheng, W. Shiyong, Z. Zetian et al., "Mining-induced mechanical response of coal and rock at different depths: a case study in the Pingdingshan mining area," *Arabian Journal of Geosciences*, vol. 13, no. 19, p. 972, 2020.

[5] L. Fei, M. Zhanguo, H. Yongsheng et al., "Deformation rules for surrounding rock in directional weakening of end roofs of thin bedrocks and ultrathick seams," *Advances in Civil Engineering*, vol. 2020, Article ID 8882374, 12 pages, 2020.

[6] T. Min, B. Qingwei, F. Baojie et al., "Mechanical analysis of mining stress transfer on isolated island face in extra-thick fully mechanized top-coal caving mining," *Geofluids*, vol. 2020, Article ID 8834321, 16 pages, 2020.

[7] Z. Anlin, Z. Ru, G. Mingzhong et al., "Failure behavior and damage characteristics of coal at different depths under triaxial unloading based on acoustic emission," *Energies*, vol. 13, no. 17, p. 4451, 2020.

[8] Y. Qiangling, Y. Liqiang, L. Xuehua et al., "The effects of micro- and meso-scale characteristics on the mechanical properties of coal-bearing sandstone," *Arabian Journal of Geosciences*, vol. 13, no. 17, p. 871, 2020.

[9] L. Minmin, L. Weimin, Y. Gaowei et al., "Dynamic mechanical properties of structural anisotropic coal under low and medium strain rates," *Plos One*, vol. 15, no. 8, p. e0236802, 2020.

[10] L. Jian, D. Zhaowen, and G. Zhongping, "Effect of high temperature (600 degrees C) on mechanical properties, mineral composition, and microfracture characteristics of sandstone," *Advances in Materials Science and Engineering*, vol. 2020, Article ID 5072534, 19 pages, 2020.

[11] Z. Yang, Y. Yongjie, and M. Depeng, "Mechanical characteristics of coal samples under triaxial unloading pressure with different test paths," *Shock and Vibration*, vol. 2020, Article ID 8870821, 10 pages, 2020.

[12] W. Tuo, M. Zhanguo, G. Peng et al., "Analysis of failure characteristics and strength criterion of coal-rock combined body with different height ratios," *Advances in Civil Engineering*, vol. 2020, Article ID 8842206, 14 pages, 2020.

[13] Q. Xinzhan, Z. Yu, and H. Manchao, "Experimental study on mechanical properties and acoustic emission characteristics of water bearing sandstone under stable cyclic loading and unloading," *Shock and Vibration*, vol. 2020, Article ID 9472656, 15 pages, 2020.

[14] W. Jie, F. Jianxin, and S. Weidong, "Mechanical properties and microstructure of layered cemented paste backfill under triaxial cyclic loading and unloading," *Construction and Building Materials*, vol. 257, p. 119540, 2020.

[15] H. Mengzhe, X. Yuanyou, L. Xiqi et al., "Evolution characteristics of temperature fields of rockburst samples under different stress gradients," *Infrared Physics & Technology*, vol. 109, p. 103425, 2020.

[16] R. Heng, Z. Yongjian, W. Ping et al., "Experimental study on mechanical characteristics of unloaded damaged white sandstone before peak," *Arabian Journal of Geosciences*, vol. 13, no. 17, p. 878, 2020.

[17] S. R. Wang, X. G. Wu, J. H. Yang, J. Q. Zhao, and F. L. Kong, "Mechanical behavior of lightweight concrete structures subjected to 3D coupled static-dynamic loads," *Acta Mechanica*, vol. 231, no. 11, pp. 4497–4511, 2020.

[18] W. Guoyin, W. Kui, Z. Mingjie et al., "Analysis of damage evolution of sandstone under uniaxial loading and unloading conditions based on resistivity characteristics," *Advances in Civil Engineering*, vol. 2019, Article ID 9286819, 12 pages, 2019.

[19] Z. Xiang, W. Kai, D. Feng et al., "Failure and seepage characteristics of gas-bearing coal under accelerated loading and unloading condition," *Applied Sciences-Basel*, vol. 9, no. 23, p. 5141, 2019.

[20] F. Wenlin, Q. Chunsheng, N. Shuangjian et al., "Macromechanical properties of saturated sandstone of Jushan Mine under post-peak cyclic loading: an experimental study," *Arabian Journal of Geosciences*, vol. 12, no. 23, p. 702, 2019.

[21] S. Wei, D. Linming, H. Hu et al., "Mechanical and coal burst breeding mechanism of coal samples under true triaxial loading and unloading," *Advances in Civil Engineering*, vol. 2019, Article ID 6050975, 15 pages, 2019.

[22] G. Yintong, W. Lei, and C. Xin, "Study on the damage characteristics of gas-bearing shale under different unloading stress paths," *Plos One*, vol. 14, no. 11, p. e0224654, 2019.

[23] D. Weisheng, Z. Kexue, and S. Huan, "Mechanical properties and energy development characteristics of impact-prone coal specimens under uniaxial cyclic loading," *Aip Advances*, vol. 9, no. 11, Article ID 115114, 2019.

[24] P. Kang, Z. Jiaqi, Z. Quanle et al., "Deformation characteristics of sandstones during cyclic loading and unloading with varying lower limits of stress under different confining pressures," *International Journal of Fatigue*, vol. 127, pp. 82–100, 2019.

[25] C. Yapei, S. Haitao, and Z. Dongming, "Experimental study on evolution in the characteristics of permeability, deformation, and energy of coal containing gas under triaxial cyclic loading-unloading," *Energy Science & Engineering*, vol. 7, no. 5, pp. 2112–2123, 2019.

[26] Y. Luo, "Influence of water on mechanical behavior of surrounding rock in hard-rock tunnels: an experimental simulation," *Engineering Geology*, vol. 277, p. 105816, 2020.

[27] X. Guangxiang, Y. Zhiqiang, W. Lei, H. Zuxiang, and C. Zhu, "Effects of gas pressure on the failure characteristics of coal," *Rock Mechanics and Rock Engineering*, vol. 50, no. 7, pp. 1711–1723, 2017.

[28] Z. Q. Yin, Z. X. Hu, Z. D. Wei et al., "Assessment of blasting-induced ground vibration in an open-pit mine under different rock properties," *Advances in Civil Engineering*, vol. 2018, Article ID 4603687, 10 pages, 2018.

[29] Z. Yin and W. Chen, H. Hao et al., "Dynamic compressive test of gas-containing coal using a modified Split Hopkinson pressure bar system," *Rock Mechanics and Rock Engineering*, vol. 53, no. 2, pp. 815–829, 2019.

[30] R. Feng, S. Chen, and S. Bryant, "Investigation of anisotropic deformation and stress-dependent directional permeability of coalbed methane reservoirs," *Rock Mechanics and Rock Engineering*, vol. 53, no. 2, pp. 625–639, 2020.

[31] Z. Tao, C. Zhu, M. He, and M. Karakus, "A physical modeling-based study on the control mechanisms of Negative Poisson's ratio anchor cable on the stratified toppling deformation of anti-inclined slopes," *International Journal of Rock Mechanics and Mining Sciences*, vol. 138, p. 104632, 2021.

[32] C. Zhu, M. He, M. Karakus, X. Zhang, and Z. Tao, "Numerical simulations of the failure process of anaclinal slope physical model and control mechanism of negative Poisson's ratio cable," *Bulletin of Engineering Geology and the Environment*, vol. 80, no. 4, pp. 3365–3380, 2021.

[33] Y. Wang, W. K. Feng, R. L. Hu, and C. H. Li, "Fracture evolution and energy characteristics during marble failure under triaxial fatigue cyclic and confining pressure unloading (FC-CPU) conditions," *Rock Mechanics and Rock Engineering*, vol. 54, no. 2, pp. 799–818, 2021.

[34] B. Li, R. Bao, Y. Wang, R. Liu, and C. Zhao, "Permeability evolution of two-dimensional fracture networks during shear under constant normal stiffness boundary conditions," *Rock Mechanics and Rock Engineering*, vol. 54, no. 3, pp. 1–20, 2021.

[35] Q. Wang, H. Gao, B. Jiang, S. Li, M. He, and Q. Qin, "In-situ test and bolt-grouting design evaluation method of underground engineering based on digital drilling," *International Journal of Rock Mechanics and Mining Sciences*, vol. 138, p. 104575, 2021.

[36] A. Li, F. Dai, Y. Liu, H. Du, and R. Jiang, "Dynamic stability evaluation of underground cavern sidewalls against flexural toppling considering excavation-induced damage," *Tunnelling and Underground Space Technology*, vol. 112, p. 103903, 2021.

[37] Z. G. Tao, C. Zhu, M. C. He, and K. M. Liu, "Research on the safe mining depth of anti-dip bedding slope in Changshanhao Mine," *Geomechanics and Geophysics for Geo-Energy and Geo-Resources*, vol. 36, no. 6, pp. 1–20, 2020.

[38] Y. Luo, F.-q. Gong, X.-b. Li, and S.-y. Wang, "Experimental simulation investigation of influence of depth on spalling characteristics in circular hard rock tunnel," *Journal of Central South University*, vol. 27, no. 3, pp. 891–910, 2020.

[39] G. Yin, C. Jiang, J. G. Wang, and J. Xu, "Geomechanical and flow properties of coal from loading axial stress and unloading confining pressure tests," *International Journal of Rock Mechanics and Mining Sciences*, vol. 76, no. 3, pp. 155–161, 2015.